Quantum parameter estimation in a dissipative environment

Wei Wu* and Chuan Shi
School of Physical Science and Technology, Lanzhou University, Lanzhou 730000, People's Republic of China

(Received 17 June 2020; accepted 17 August 2020; published 8 September 2020)

We investigate the performance of quantum parameter estimation based on a qubit probe in a dissipative bosonic environment beyond the traditional paradigm of weak-coupling and rotating-wave approximations. By making use of an exactly numerical hierarchical equations of motion method, we analyze the influences of the non-Markovian memory effect induced by the environment and the form of probe-environment interaction on the estimation precision. It is found that (i) the non-Markovianity can effectively boost the estimation performance and (ii) the estimation precision can be improved by introducing a perpendicular probe-environment interaction. Our results indicate the scheme of parameter estimation in a noisy environment can be optimized via engineering the decoherence mechanism.

DOI: 10.1103/PhysRevA.102.032607

I. INTRODUCTION

Ultrasensitive parameter estimation plays an important role in both theoretical and practical researches. It has wide applications from gravitational wave detection [1,2] and atom clock synchronization [3,4] to various high accuracy thermometries [5–7] and magnetometers [8–10]. Many previous studies have revealed that certain quantum resources, for example, entanglement [11–14] and quantum squeezing [15,16], can substantially improve the estimation precision and beat the shot-noise limit (standard quantum limit), which is set by the law of classical statistics. Thus, using quantum technology to attain a higher estimation accuracy has became a hot topic in the last decades, and the theory of quantum parameter estimation has been established correspondingly [17,18]. Quantum Fisher information (QFI) lies at the heart of quantum parameter estimation [19–21]. Roughly speaking, it characterizes the statistical information which is extractable from a quantum state carrying the parameter of interest. In this sense, QFI theoretically determines the minimal estimation error, which is independent of specific measurement schemes. Moreover, going beyond the scope of quantum estimation theory, it has been revealed that QFI can be also used to detect the quantum phase transition of a many-body system [22–25], quantify the smallest evolution time for a quantum process [26–28], and measure the non-Markovian information flow in an open quantum system [29–31].

In any practical and actual parameter estimation scheme, the quantum probe, carrying the parameter of interest, unavoidably interacts with its surrounding environment, which generally impairs the quantum resource labeling on the probe and induces the deterioration of quantum coherence. In this sense, the probe and its surrounding environment form an open quantum system [32–34], which implies the estimation performance can be severely influenced by the environment. To gain a global view and more physical insight into the quantum parameter estimation problem, the estimation scheme should be investigated within the framework of quantum dissipative dynamics and how to degrade the noise's impact should be taken into account [35–38]. Almost all the existing studies of parameter estimation in a noisy environment restricted their attentions to some exactly solvable situations. For example, they usually assume the probe suffers a pure dephasing decoherence channel [39,40] or certain especial amplitude-damping decoherence channels [41–45]. Very few studies focus on the more general case, where both the dephasing mechanism and quantum relaxation are considered. Considering the fact that the real decoherence process is intricate, generalizing the study of noisy parameter estimation to a more general dissipative environment is highly desirable from both theoretical and experimental perspectives.

To address the above concern, one needs to solve the difficulty in achieving an accurate dynamical description of the quantum probe, which is coupled to a general dissipative environment. Therefore, an efficient and reliable approach is typically required. In this paper, we adopt the hierarchical equations of motion (HEOM) approach [46–50] to handle this problem. The HEOM is a set of time-local differential equations for the reduced density matrix of the probe, which can provide a completely equivalent description of the exact Schrödinger equation (or the quantum von Neumann equation). This method is beyond the usual Markovian approximation, the rotating-wave approximation (RWA), and the perturbative approximation. Thus, the HEOM can be viewed as an exactly numerical treatment of the quantum dissipative dynamics. In recent years, the HEOM approach has been successfully used to study the anomalous decoherence phenomenon in a nonlinear spin-boson model [51], the quantum Zeno and anti-Zeno phenomena in a noisy environment [52], as well as the influence of counter-rotating-wave terms on the measure of non-Markovianity [53].

*wuw@lzu.edu.cn

 ©2020 American Physical Society

In this paper, we employ the HEOM method to study the quantum parameter estimation problem in a general dissipative environment. In Sec. II, we briefly outline some basic concepts as well as the general formalism of quantum parameter estimation. In Sec. III, we present three different methods employed in this paper in detail, including the HEOM approach, the general Bloch equation (GBE) technique [54,55], and the RWA treatment. Compared with the RWA approach, the effect of counter-rotating-wave terms is considered in the GBE method. Thus it can be employed as a benchmark of the purely numerical HEOM approach. The main results and the conclusions of this paper are drawn in Secs. IV and V, respectively. Throughout the paper, we set $\hbar = k_{\rm B} = 1$ for the sake of simplicity, and all the other units are dimensionless as well.

II. NOISY QUANTUM PARAMETER ESTIMATION

In the theory of quantum parameter estimation, the parameter's information is commonly encoded into the state of the quantum probe via a unitary [56–58] or nonunitary dynamics [39–45,59–61]. Then, one can extract the message of the parameter θ from the output state of the probe ρ_θ via repeated quantum measurements. In such quantum parameter estimation process, one cannot completely eliminate all the errors and estimate θ precisely. There exists a minimal estimation error, which cannot be removed by optimizing the estimation scheme and is given by the famous quantum Cramér-Rao bound [19–21]:

$$\delta\theta \geqslant \frac{1}{\sqrt{\upsilon F(\theta)}}, \tag{1}$$

where $\delta\theta$ the root mean square of θ, υ is the number of repeated measurements (in this paper, we set $\upsilon = 1$ for the sake of convenience), and $F(\theta) \equiv \mathrm{Tr}(\rho_\theta \hat{L}_\theta)$ with $\hat{L}_\theta$ determined by $\partial_\theta \rho_\theta = \frac{1}{2}(\hat{L}_\theta \rho_\theta + \rho_\theta \hat{L}_\theta)$ is the QFI with respect to the output state ρ_θ. From Eq. (1), one can immediately find that the optimal estimation precision is completely decided by the value of QFI: the larger the QFI, the smaller the estimation error is. How to saturate the smallest theoretical error (or boost the QFI) is the most crucial problem in the field of quantum parameter estimation.

To compute the QFI from the θ-dependent density operator ρ_θ, one first needs to diagonalize ρ_θ as $\rho_\theta = \sum_\ell \xi_\ell |\xi_\ell\rangle\langle\xi_\ell|$, where $\xi_\ell \equiv \xi_\ell(\theta)$ and $|\xi_\ell\rangle \equiv |\xi_\ell(\theta)\rangle$ are eigenvalues and eigenvectors of ρ_θ, respectively. Then, the QFI can be computed as [21]

$$F(\theta) = \sum_\ell \frac{(\partial_\theta \xi_\ell)^2}{\xi_\ell} + \sum_\ell 4\xi_\ell \langle \partial_\theta \xi_\ell | \partial_\theta \xi_\ell \rangle - \sum_{\ell,\ell'} \frac{8\xi_\ell \xi_{\ell'}}{\xi_\ell + \xi_{\ell'}} |\langle \partial_\theta \xi_\ell | \xi_{\ell'} \rangle|^2. \tag{2}$$

Specially, for a two-dimensional density operator described in the Bloch representation, namely, $\rho_\theta = \frac{1}{2}(\mathbf{1}_2 + \langle \hat{\underline{\sigma}} \rangle \cdot \hat{\boldsymbol{\sigma}})$ with $\langle \hat{\underline{\sigma}} \rangle \equiv (\langle \hat{\sigma}_x \rangle, \langle \hat{\sigma}_y \rangle, \langle \hat{\sigma}_z \rangle)^{\mathbb{T}}$ being the Bloch vector and $\hat{\boldsymbol{\sigma}} \equiv (\hat{\sigma}_x, \hat{\sigma}_y, \hat{\sigma}_z)$ being the vector of Pauli matrices, Eq. (2) can be further simplified to [21]

$$F(\theta) = |\partial_\theta \langle \hat{\underline{\sigma}} \rangle|^2 + \frac{(\langle \hat{\underline{\sigma}} \rangle \cdot \partial_\theta \langle \hat{\underline{\sigma}} \rangle)^2}{1 - |\langle \hat{\underline{\sigma}} \rangle|^2}. \tag{3}$$

For the pure-state case, the above equation reduces to $F(\theta) = |\partial_\theta \langle \hat{\underline{\sigma}} \rangle|^2$. Compared with Eq. (2), Eq. (3) is more computable in practice, because it avoids the operation of diagonalization.

In this paper, we assume a qubit, acting as the probe and carrying the parameter of interest, is linearly coupled to a dissipative environment. The Hamiltonian of the quantum probe is described by $\hat{H}_{\rm s} = \frac{1}{2}\Delta\hat{\sigma}_x$, where Δ represents the frequency of tunneling between the two levels of the qubit and *is the encoded parameter to be estimated in this paper*. We assume the dissipative environment is stimulated by a set of harmonic oscillators, i.e., $\hat{H}_{\rm b} = \sum_k \omega_k \hat{b}_k^\dagger \hat{b}_k$, where $\hat{b}_k^\dagger$ and $\hat{b}_k$ are the creation and annihilation operators of the kth harmonic oscillator with corresponding frequency ω_k, respectively. Thus, the Hamiltonian of the whole qubit probe plus the environment is given by $\hat{H} = \hat{H}_{\rm s} + \hat{H}_{\rm b} + \hat{H}_{\rm i}$. Here, we assume the probe-environment interaction part can be described in the following linear form:

$$\hat{H}_{\rm i} = \hat{\mathcal{S}} \otimes \hat{\mathcal{B}}, \tag{4}$$

where $\hat{\mathcal{S}}$ denotes the probe's operator coupled to its surrounding environment, and $\hat{\mathcal{B}} \equiv \sum_k g_k(\hat{b}_k^\dagger + \hat{b}_k)$ with g_k being the coupling strength between the probe and the kth environmental mode.

After a period of nonunitary dynamics, the information of Δ is then encoded in the reduced density operator of the probe, namely, $\varrho_{\rm s}(t) \equiv \mathrm{Tr}_{\rm b}[e^{-i\hat{H}t}\varrho_{\rm sb}(0)e^{i\hat{H}t}]$. Here, $\varrho_{\rm sb}(0)$ is the initial state of the whole Hamiltonian. Generally speaking, the ultimate estimation precision associated with $\varrho_{\rm s}(t)$ depends on a number of factors. In this paper, we concentrate on the following two elements: *the characteristic of the environment* and *the form of the probe-environment coupling operator*. The property of the environment is mainly reflected by the environmental autocorrelation function, which is defined by

$$\alpha(t) \equiv \mathrm{Tr}_{\rm b}(e^{it\hat{H}_{\rm b}}\hat{\mathcal{B}}e^{-it\hat{H}_{\rm b}}\hat{\mathcal{B}}\varrho_{\rm b}), \tag{5}$$

with $\varrho_{\rm b}$ being the initial state of the environment. Thus, we shall discuss the effect of $\alpha(t)$ and $\hat{\mathcal{S}}$ on the QFI with respect to $\varrho_{\rm s}(t)$. The determination of the QFI requires the knowledge of the reduced density operator $\varrho_{\rm s}(t)$. Unfortunately, except in a few special situations, the exact expression of $\varrho_{\rm s}(t)$ is generally difficult to obtain. To overcome this difficulty, we would like to adopt the following three different methods to evaluate $F(\Delta)$.

III. METHODOLOGY

In this section, we introduce the dynamical formulations employed in our paper. The first one is the HEOM method, which can provide rigorous numerical results. As comparisons, we also present two analytical methods: the GBE and the RWA approaches. In this paper, we assume the initial state of the whole probe-environment system has a factorizing form, i.e., $\varrho_{\rm sb}(0) = \varrho_{\rm s}(0) \otimes \varrho_{\rm b}$, where $\varrho_{\rm b} = |\mathbf{0}_k\rangle\langle\mathbf{0}_k|$ with $|\mathbf{0}_k\rangle \equiv \bigotimes_k |0_k\rangle$ being the Fock vacuum state of the environment.

A. HEOM

The HEOM can be viewed as a bridge linking the well-known Schrödinger equation, which is exact but generally difficult to solve straightforwardly, and a set of ordinary differential equations, which can be handled numerically by using the Runge-Kutta method. How to establish such a connection, which should be elaborately designed and avoid losing any important dynamical feature of the quantum probe, is the most important step in the HEOM treatment [62,63]. In many previous references, the HEOM algorithm is realized by making use of the path-integral influence functional approach [48,49]. In this paper, we establish the HEOM in an alternative way: within the framework of the non-Markovian quantum state diffusion approach [62,64,65].

The dynamics of $\hat{H}$ is determined by the Schrödinger equation $\partial_t|\Psi_{\rm sb}(t)\rangle = -i\hat{H}|\Psi_{\rm sb}(t)\rangle$, where $|\Psi_{\rm sb}(t)\rangle$ is the pure-state wave function of the whole probe-environment system. Any straightforward treatment of the above Schrödinger equation can be rather troublesome, because of the large number of degrees of freedom. However, by employing the bosonic coherent state, which is defined by $|\mathbf{z}\rangle = \bigotimes_k |z_k\rangle$ with $|z_k\rangle \equiv e^{z_k\hat{b}_k^\dagger}|0_k\rangle$, one can recast the original Schrödinger equation into the following stochastic quantum state diffusion equation (see the Appendix for more details):

$$\frac{\partial}{\partial t}|\psi_t(\mathbf{z}^*)\rangle = -i\hat{H}_{\rm s}|\psi_t(\mathbf{z}^*)\rangle + \hat{\mathcal{S}}\mathbf{z}_t^*|\psi_t(\mathbf{z}^*)\rangle - \hat{\mathcal{S}}\int_0^t d\tau\alpha(t-\tau)\frac{\delta}{\delta\mathbf{z}_\tau^*}|\psi_t(\mathbf{z}^*)\rangle, \tag{6}$$

where $|\psi_t(\mathbf{z}^*)\rangle \equiv \langle\mathbf{z}|\Psi_{\rm sb}(t)\rangle$ is the total pure-state wave function in the coherent-state representation, the variable $\mathbf{z}_t \equiv i\sum_k g_k z_k e^{-i\omega_k t}$ can be regarded as a stochastic Gaussian colored noise satisfying $\mathcal{M}\{\mathbf{z}_t\} = \mathcal{M}\{\mathbf{z}_t^*\} = 0$, and $\mathcal{M}\{\mathbf{z}_t\mathbf{z}_\tau^*\} = \alpha(t-\tau)$. Here $\mathcal{M}\{...\}$ denotes the statistical mean over all the possible quantum trajectories, and $\alpha(t) = \sum_k g_k^2 e^{-i\omega_k t}$ is the autocorrelation function at zero temperature. In this paper, we concentrate on an Ornstein-Uhlenbeck-type autocorrelation function, namely,

$$\alpha(t) = \tfrac{1}{2}\Gamma\gamma e^{-\gamma t}, \tag{7}$$

where Γ can be viewed as the probe-environment coupling strength and γ is connected to the memory time of the environment.

Notice that the autocorrelation function has an exponential form of time, which means $\partial_t\alpha(t) = -\gamma\alpha(t)$. Using this property, we can replace the stochastic quantum state diffusion equation in Eq. (6) with a set of hierarchial equations of the pure-state wave function $|\psi_t(\mathbf{z}^*)\rangle$ as follows [62,64,65]:

$$\frac{\partial}{\partial t}\left|\psi_t^{(m)}\right\rangle = (-i\hat{H}_{\rm s} - m\gamma + \hat{\mathcal{S}}\mathbf{z}_t^*)\left|\psi_t^{(m)}\right\rangle + \frac{1}{2}m\Gamma\gamma\hat{\mathcal{S}}\left|\psi_t^{(m-1)}\right\rangle - \hat{\mathcal{S}}\left|\psi_t^{(m+1)}\right\rangle, \tag{8}$$

where

$$\left|\psi_t^{(m)}\right\rangle \equiv \left[\int_0^t d\tau C(t-\tau)\frac{\delta}{\delta\mathbf{z}_\tau^*}\right]^m|\psi_t(\mathbf{z}^*)\rangle$$

are auxiliary pure-state wave functions. The hierarchy equation of $|\psi_t(\mathbf{z}^*)\rangle$ in Eq. (8) no longer contains functional derivatives, but still has stochastic noise terms which hinder the efficiency of numerical simulation. To extract a deterministic equation of motion for the reduced density operator, one needs to trace out the degrees of freedom of the environment by taking the statistical mean over all the possible quantum trajectories [62,63]. The expression of the reduced density operator is then given by $\varrho_{\rm s}(t) = \varrho_t \equiv \mathcal{M}\{|\psi_t(\mathbf{z}^*)\rangle\langle\psi_t(\mathbf{z}^*)|\}$. As shown in Ref. [62], the equation of motion for ϱ_t can be derived from Eq. (8), and reads

$$\frac{d}{dt}\varrho_t^{(m,n)} = -i\left[\hat{H}_{\rm s}, \varrho_t^{(m,n)}\right] - \gamma(m+n)\varrho_t^{(m,n)} + \frac{1}{2}\Gamma\gamma\left[m\hat{\mathcal{S}}\varrho_t^{(m-1,n)} + n\varrho_t^{(m,n-1)}\hat{\mathcal{S}}\right] - \left[\hat{\mathcal{S}}, \varrho_t^{(m+1,n)}\right] + \left[\hat{\mathcal{S}}, \varrho_t^{(m,n+1)}\right], \tag{9}$$

where $\varrho_t^{(m,n)} \equiv \mathcal{M}\{|\psi_t^{(m)}(\mathbf{z}^*)\rangle\langle\psi_t^{(n)}(\mathbf{z}^*)|\}$ are auxiliary reduced density operators. Equation (9) is nothing but a set of ordinary differential equations, which shall be handled in our numerical simulations.

The initial-state conditions of the auxiliary operators are $\varrho_t^{(0,0)} = \varrho_{\rm s}(0)$ and $\varrho_t^{(m>0,n>0)} = 0$. In numerical simulations, we need to truncate the hierarchical equations by choosing a sufficiently large integer N. All the terms of $\varrho_t^{(m,n)}$ with $m+n > N$ are set to zero, while the terms of $\varrho_t^{(m,n)}$ with $m+n \leqslant N$ consist of a closed set of ordinary differential equations which can be solved directly by using the fourth-order Runge-Kutta method. It is necessary to emphasize that no approximation is invoked in the above derivation from Eq. (6) to Eq. (9), which means the mapping from the original Schrödinger equation to the hierarchy equations given by Eq. (9) is exact. In this sense, the numerics obtained from Eq. (9) should be viewed as rigorous results.

B. GBE

If $\hat{\mathcal{S}} = \hat{\sigma}_z$, Eq. (4) has a purely transversal or perpendicular interaction (recalling that $\hat{H}_{\rm s} = \frac{1}{2}\Delta\hat{\sigma}_x$). Thus, the probe-environment system has the same structure as the famous spin-boson model, which leads to both the loss of information and the dissipation of energy. The equation of motion of the spin-boson model is governed by the quantum von Neumann equation $\partial_t\varrho_{\rm sb}(t) = -i[\hat{H}, \varrho_{\rm sb}(t)]$, which provides an exact dynamical prediction. Applying Zwanzig's projection technique with the Born approximation, the quantum von Neumann equation can be transformed to the well-known Zwanzig-Nakajima master equation [66,67]

$$\frac{\partial}{\partial t}\varrho_{\rm s}(t) = -i\hat{\mathcal{L}}_{\rm s}\varrho_{\rm s}(t) - \int_0^t d\tau\hat{\Sigma}(t-\tau)\varrho_{\rm s}(\tau), \tag{10}$$

where $\hat{\Sigma}(t)$ is the self-energy superoperator:

$$\hat{\Sigma}(t) = {\rm Tr}_{\rm b}\left[\hat{\mathcal{L}}_{\rm i}e^{-it\hat{\mathcal{Q}}(\hat{\mathcal{L}}_{\rm s}+\hat{\mathcal{L}}_{\rm b}+\hat{\mathcal{L}}_{\rm i})}\hat{\mathcal{L}}_{\rm i}\varrho_{\rm b}\right], \tag{11}$$

where $\hat{\mathcal{L}}_{\rm x}$ with ${\rm x} = {\rm s}, {\rm b}, {\rm i}$ is the Liouvillian superoperator satisfying $\hat{\mathcal{L}}_{\rm x}\hat{\mathcal{O}} = [\hat{H}_{\rm x}, \hat{\mathcal{O}}]$, and $\hat{\mathcal{Q}} \equiv 1 - \varrho_{\rm b}{\rm Tr}_{\rm b}$ is Zwanzig's projection superoperator. From Eq. (10), one can notice the evolution of $\varrho_{\rm s}(t)$ depends on $\varrho_{\rm s}(\tau)$ at all the earlier times

$0 < \tau < t$, implying the memory effect from the environment has been considered and is incorporated into the self-energy superoperator $\hat{\Sigma}(t-\tau)$. Thus, the result from Eq. (9) is then non-Markovian.

The exact treatment of the above Zwanzig-Nakajima master equation in Eq. (10) is challenging. Fortunately, the self-energy superoperator of Eq. (11) can be expanded in powers of the interaction Liouvillian $\hat{\mathcal{L}}_{\rm i}$. Only retaining the lowest-order term in the series, $\hat{\Sigma}(t)$ can be approximated as [54,55,68]

$$\hat{\Sigma}(t) \simeq \mathrm{Tr}_{\rm b}\big[\hat{\mathcal{L}}_{\rm i} e^{-it(\hat{\mathcal{L}}_{\rm s}+\hat{\mathcal{L}}_{\rm b})}\hat{\mathcal{L}}_{\rm i}\varrho_{\rm b}\big]. \tag{12}$$

Equation (10) together with the approximate $\hat{\Sigma}(t)$ in Eq. (12) constitute a general non-Markovian quantum master equation, which has been widely used in many previous studies [54,55,69].

By introducing the time-dependent Bloch vector $\langle\hat{\underline{\sigma}}(t)\rangle$ with $\langle\hat{\sigma}_i(t)\rangle \equiv \mathrm{Tr}_{\rm s}[\hat{\sigma}_i\varrho_{\rm s}(t)]$, one can rewrite the above general quantum master equation as the following GBE [54,55]:

$$\frac{d}{dt}\langle\hat{\underline{\sigma}}(t)\rangle = \hat{\mathfrak{T}}(t)\diamond\langle\hat{\underline{\sigma}}(t)\rangle, \tag{13}$$

where $\diamond$ denotes the convolution and

$$\hat{\mathfrak{T}}(t) = \begin{bmatrix} -\mathfrak{A}(t) & 0 & 0 \\ 0 & -\mathfrak{B}(t) & -\Delta\delta(t) \\ 0 & \Delta\delta(t) & 0 \end{bmatrix},$$

with $\mathfrak{A}(t) = 4\cos(\Delta t)\alpha(t)$, $\mathfrak{B}(t) = 4\alpha(t)$. By means of the Laplace transform, one can find

$$\begin{aligned}\langle\hat{\sigma}_i(\lambda)\rangle &\equiv \int_0^\infty dt\,\langle\hat{\sigma}_i(t)\rangle e^{-\lambda t} \\ &= \sum_j \mathfrak{F}_{ij}(\lambda)\langle\hat{\sigma}_j(0)\rangle,\end{aligned} \tag{14}$$

where $i, j = x, y, z$. For the perpendicular probe-environment interaction case, the nonvanishing terms of $\mathfrak{F}_{ij}(\lambda)$ are

$$\begin{aligned}\mathfrak{F}_{xx}(\lambda) &= [\lambda + \mathfrak{A}(\lambda)]^{-1}, \\ \mathfrak{F}_{yy}(\lambda) &= \left[\lambda + \mathfrak{B}(\lambda) + \frac{\Delta^2}{\lambda}\right]^{-1}, \\ \mathfrak{F}_{zz}(\lambda) &= \lambda^{-1}[\lambda + \mathfrak{B}(\lambda)]\mathfrak{F}_{yy}(\lambda), \\ \mathfrak{F}_{yz}(\lambda) &= -\mathfrak{F}_{zy}(\lambda) = -\Delta\lambda^{-1}\mathfrak{F}_{yy}(\lambda).\end{aligned}$$

Then, for an arbitrary given initial state $\langle\hat{\underline{\sigma}}(0)\rangle$, the dynamics of $\langle\hat{\underline{\sigma}}(t)\rangle$ can be completely determined by the GBE method in Eq. (14) with the help of the inverse Laplace transform.

C. RWA

For the purely perpendicular interaction case, one can use an alternative method, the RWA approach, to obtain the dynamical behavior of the probe. The RWA can remove the counter-rotating-wave terms in $\hat{H}$ and obtain the following approximate Hamiltonian:

$$\hat{H}_{\rm RWA} = \frac{\Delta}{2}\hat{\sigma}_x + \sum_k \omega_k \hat{b}_k^\dagger \hat{b}_k + \sum_k g_k(\hat{\sigma}_-\hat{b}_k^\dagger + \hat{\sigma}_+\hat{b}_k), \tag{15}$$

where $\hat{\sigma}_+ \equiv |+\rangle\langle -|$ and $\hat{\sigma}_- \equiv |-\rangle\langle +|$ with $|\pm\rangle$ being the eigenvectors of $\hat{\sigma}_x$, i.e., $\hat{\sigma}_x|\pm\rangle = \pm|\pm\rangle$. The Hamiltonian $\hat{H}_{\rm RWA}$ commutes with the total excitation number operator $\hat{\mathcal{N}} = \hat{\sigma}_+\hat{\sigma}_- + \sum_k \hat{b}_k^\dagger\hat{b}_k$, which is thus a constant of motion and can greatly simplify the reduced dynamical solution of the probe in this situation.

At zero temperature, the reduced dynamics of the probe is exactly solvable in the RWA case and can be conveniently expressed in the basis of $\{|+\rangle, |-\rangle\}$ as follows:

$$\varrho_{\rm s}(t) = \begin{bmatrix} \varrho_{++}(0)\mathcal{G}_t^2 & \varrho_{+-}(0)\mathcal{G}_t e^{-i\Delta t} \\ \varrho_{-+}(0)\mathcal{G}_t e^{i\Delta t} & 1-\varrho_{++}(0)\mathcal{G}_t^2 \end{bmatrix}, \tag{16}$$

where $\mathcal{G}_t$ is the decay factor. For the Ornstein-Uhlenbeck-type autocorrelation function considered in this paper, the exact expression of $\mathcal{G}_t$ is given by [53]

$$\mathcal{G}_t = \exp\left(-\frac{1}{2}\gamma t\right)\left[\cosh\left(\frac{1}{2}\Omega t\right) + \frac{\gamma}{\Omega}\sinh\left(\frac{1}{2}\Omega t\right)\right], \tag{17}$$

with $\Omega \equiv \sqrt{\gamma^2 - 2\gamma\Gamma}$. As shown in many previous studies [50,53], the RWA is acceptable in the weak probe-environment coupling regime, and we thus expect it can provide a reasonable prediction in the above region.

D. Comparison

In Fig. 1, we display the dynamics of the population difference $\langle\hat{\sigma}_z(t)\rangle$ of the qubit probe, which is a very common quantity of interest in experiments. For the RWA case, the exact expression of the population difference $\langle\hat{\sigma}_z(t)\rangle$ is given by $\langle\hat{\sigma}_z(t)\rangle_{\rm RWA} = \mathcal{G}_t\cos(\Delta t)$.

For the Ornstein-Uhlenbeck-type correlation function considered in this paper, the boundary between Markovian and non-Markovian regimes can be approximately specified by the ratio of γ/Γ [52,70]. When γ/Γ is large, the correlation function reduces to a delta correlated autocorrelation function, i.e., $\alpha(t-\tau) \simeq \Gamma\delta(t-\tau)$, which means the environment is memoryless and the decoherence dynamics is Markovian. On the contrary, if γ/Γ is small, the environmental memory effect cannot be neglected and the corresponding decoherence is then non-Markovian. In fact, when $\gamma/\Gamma \to \infty$, one can demonstrate that the hierarchical equations in Eq. (8) can reduce to the common Markovian Lindblad-type master equation by only considering the zeroth order of the terminator [64]. The relation between γ/Γ and the degree of non-Markovianity has been studied by making use of trace distance [71,72] and dynamical divisibility [73], and these studies are consistent with our above analysis.

We first consider the Markovian case, say $\lambda/\Gamma = 10$ in Fig. 1(a). A good agreement is found between results from the HEOM and the GBE, while the prediction from the RWA exhibits a small deviation from the above two approaches. Such deviation disappears if the probe-environment coupling becomes further weaker. Thus, three different approaches present a consistent result in Markovian and weak-coupling regimes. In the non-Markovian regime, the result from the GBE can still be in qualitative agreement with that of the numerical HEOM method if the coupling strength is weak [see Fig. 1(c)]. However, when the coupling becomes stronger,

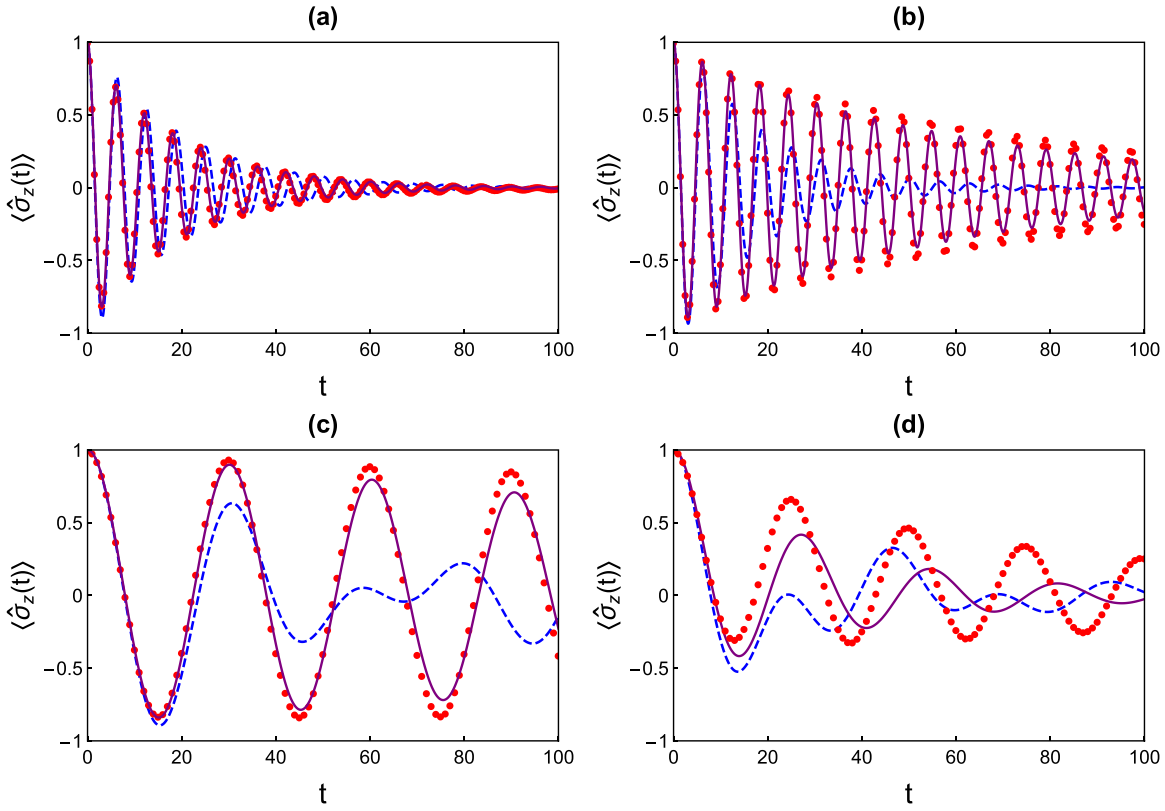

FIG. 1. The dynamics of the population difference $\langle\hat{\sigma}_z(t)\rangle$ with $\langle\hat{\sigma}_z(0)\rangle = 1$. The purple solid lines are exact numerical simulations from the HEOM method, the red circles are results from the GBE approach, and the blue dashed lines are obtained under the assumption of RWA. Parameters are chosen as (a) $\gamma = 10\Gamma$, $\Gamma = 0.1$, and $\Delta = 1$; (b) $\gamma = 4\Gamma$, $\Gamma = 0.1$, and $\Delta = 1$; (c) $\gamma = 0.2\Gamma$, $\Gamma = 0.1$, and $\Delta = 0.2$; and (d) $\gamma = 0.2\Gamma$, $\Gamma = 0.25$, and $\Delta = 0.2$.

such as the parameters chosen in Fig. 1(d), the GBE exhibits a relatively large deviation compared with the result from HEOM, probably because it neglects the higher-order terms of the probe-environment coupling. On the contrary, the result calculated with RWA gives a qualitatively incorrect conclusion in the entire non-Markovian regime, unless one only focuses on the short-time behavior of the population difference.

IV. RESULTS

In this section, we study the influence of $\alpha(t)$ and $\hat{\mathcal{S}}$ on the estimation precision of Δ in a dissipative environment. During the numerical calculations to the exact QFI using the HEOM method, one needs to handle the first-order derivative to the parameter Δ, namely, $\partial_\Delta\langle\hat{\sigma}_i(t)\rangle$ [see Eq. (3)]. In this paper, the derivative for an arbitrary θ-dependent function f_θ is numerically performed by adopting the following finite difference method:

$$\frac{\partial f_\theta}{\partial\theta} \simeq \frac{-f_{\theta+2\epsilon} + 8f_{\theta+\epsilon} - 8f_{\theta-\epsilon} + f_{\theta-2\epsilon}}{12\epsilon}. \tag{18}$$

In our numerical simulations, we set $\epsilon/\theta = 10^{-5}$, which provides a very good accuracy for finite-difference approximations. In this section, we assume the initial state of the quantum probe is given by $\frac{1}{\sqrt{2}}(|+\rangle + |-\rangle)$.

A. Effect of non-Markovianity

We first study the environmental memory effect on the noisy estimation precision. As discussion in Sec. III D, by manipulating the ratio of γ/Γ, the degree of non-Markovianity in the decoherence channel changes drastically. This feature is beneficial for us to explore the connection between the non-Markovianity and the estimation precision in a dissipative environment.

In the RWA case, one can derive a very simple expression of the QFI with respect to the parameter Δ as $F_{\mathrm{RWA}}(\Delta) = t^2\mathcal{G}_t^2$. With this expression at hand, it is very easy to check that the value of QFI can be boosted by decreasing the ratio of γ/Γ. This result implies the non-Markovianity may increase the estimation precision, which is in agreement with the results of Refs. [39,41]. Moreover, in the non-Markovian regime, we observe that the QFI oscillates with time and exhibits a collapse-and-revival phenomenon before complete disappearance. The same result is also reported in Ref. [41], and can be regarded as an evidence of reversed information flow from the environment back to the probe. Going beyond the RWA, the numerical performances from the GME and the HEOM tell us the same conclusion [see Figs. 2(b) and 2(c)]. Thus, one can conclude that the environmental non-Markovian effect can effectively improve the estimation precision regardless of whether the counter-rotating-wave terms are taken into account. In this sense, our result is a

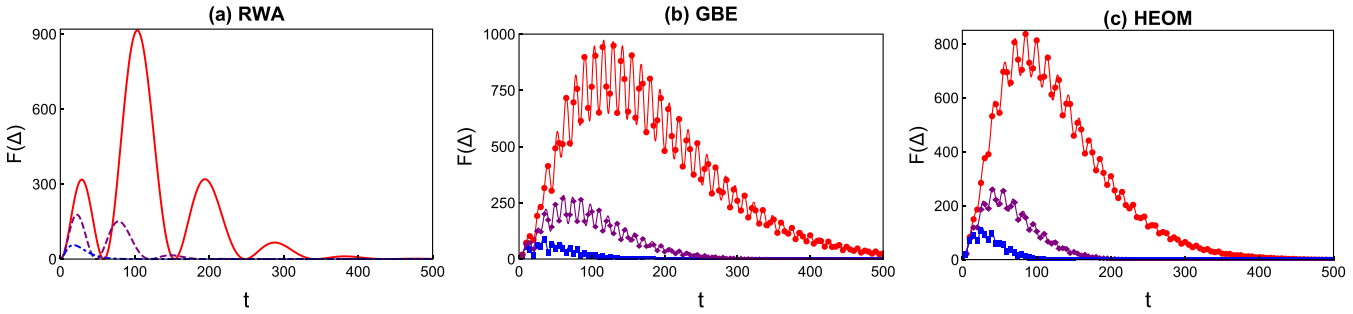

FIG. 2. (a) The QFI $F(\Delta)$ is plotted as a function of time in the RWA case. Parameters are chosen as $\gamma = 0.25\Gamma$ (red solid line), $\gamma = 0.5\Gamma$ (purple dashed line), and $\gamma = 5\Gamma$ (blue dot-dashed line) with $\Gamma = 0.1$ and $\Delta = 1$. (b) The QFI $F(\Delta)$ from the GBE method. Parameters are chosen as $\gamma = 0.25\Gamma$ (red circles), $\gamma = 0.35\Gamma$ (purple rhombuses), and $\gamma = 0.5\Gamma$ (blue rectangles) with $\Gamma = 0.2$ and $\Delta = 0.2$. (c) The QFI obtained by the numerical HEOM method. Parameters are chosen as $\gamma = 0.25\Gamma$ (red circles), $\gamma = 0.4\Gamma$ (purple rhombuses), and $\gamma = 0.6\Gamma$ (blue rectangles) with $\Gamma = 0.15$ and $\Delta = 0.2$.

nontrivial generalization of Ref. [41] in which only the RWA case is considered.

B. Dephasing versus relaxation

Generally speaking, the specific form of the probe-environment operator $\hat{\mathcal{S}}$ fully determines the decoherence channel. When $[\hat{\mathcal{S}}, \hat{H}_s] = 0$, the probe suffers a pure dephasing decoherence mechanism and only off-diagonal elements of $\varrho_s(t)$ decay during the time evolution. If $[\hat{\mathcal{S}}, \hat{H}_s] \neq 0$, the decoherence channel of the probe is relaxation, which results in the dissipation of the qubit's energy. An interesting question arises here: what is the influence of the type of decoherence channel on the estimation performance? To address this problem, we generalize our discussion to a more general situation $\hat{\mathcal{S}} = \hat{\sigma}_x + \chi\hat{\sigma}_z$, where χ is a tunable real parameter [74]. Here, both parallel interaction case $\chi = 0$ and perpendicular

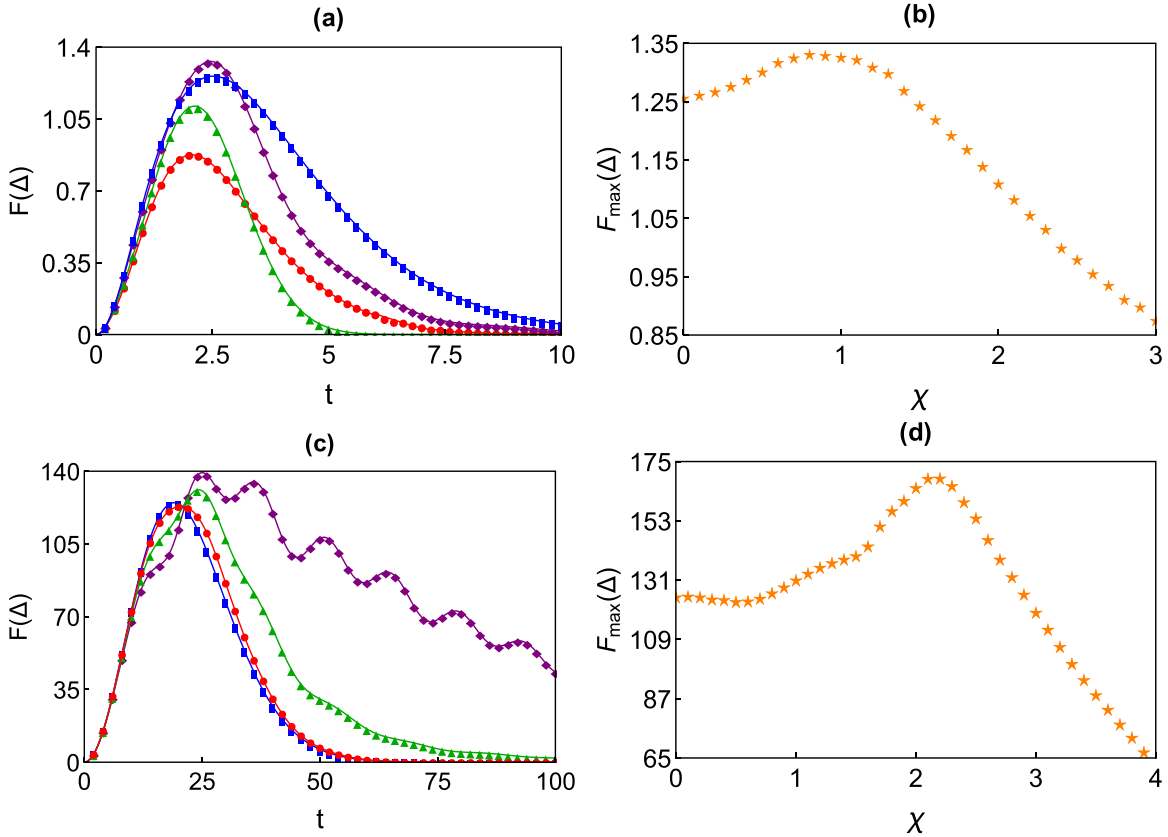

FIG. 3. (a) The QFI $F(\Delta)$ is plotted as a function of t by making use of the HEOM method with different values of χ: $\chi = 0$ (blue rectangles), $\chi = 0.75$ (purple rhombuses), $\chi = 2$ (green triangles), and $\chi = 3$ (red circles). (b) The maximum QFI with respect to time vs χ. Parameters are chosen as $\gamma = 10\Gamma$, $\Gamma = 0.2\Delta$, and $\Delta = 1$. (c) The QFI $F(\Delta)$ is displayed as a function of t in the non-Markovian regime with different values of χ: $\chi = 0$ (blue rectangles), $\chi = 1.5$ (purple rhombuses), $\chi = 1$ (green triangles), and $\chi = 0.5$ (red circles). (d) The maximum QFI vs χ in the non-Markovian regime. Parameters are chosen as $\gamma = 0.3\Gamma$, $\Gamma = 0.3\Delta$, and $\Delta = 0.25$.

interaction case $\chi \neq 0$ are included in the above expression of $\hat{\mathcal{S}}$, which can give rise to a much richer decoherence phenomenon. Such $\hat{\mathcal{S}}$ can be physically realized in an atomic gas or quantum dot system, in which the atoms or electron spins are relaxed by their surrounding phonons (say, spontaneous emission process), meanwhile the dephasing process is generated by the random fluctuations of an external electromagnetic field [75,76].

Making use of the HEOM approach, which is independent of the specific form of operator $\hat{\mathcal{S}}$, we can numerically obtain the value of QFI. From Fig. 3, we find the influence of χ on the QFI is not evident in the short-time regime. However, as time increases, the effect of χ becomes no longer negligible. Maximizing the QFI over time, one can see the maximum QFI $F_{\max}(\Delta)$ is quite sensitive to the value of χ: when χ is small, the introduction of the perpendicular interaction is favorable for obtaining a larger $F_{\max}(\Delta)$; after reaching a local maximum value, $F_{\max}(\Delta)$ gradually decreases as χ further increases. This result implies that the pure dephasing decoherence mechanism is *not* the best choice for obtaining the maximum precision estimation, which is consistent with the result reported in Ref. [61]. From Figs. 3(b) and 3(d), one can observe that $F_{\max}(\Delta)$ can be smaller than that of the pure dephasing case in the large-χ regime, which suggests there exists an optimal χ maximizing the value of QFI. Thus, we draw a conclusion that the performance of noisy parameter estimation can be enhanced by engineering the form of probe-environment coupling.

V. SUMMARY

In summary, by employing the HEOM method, we have investigated the ultimate achievable limit to a qubit probe's frequency estimation in a dissipative bosonic environment. Compared with two other approaches, it is found that the non-Markovian memory effect induced by the environment can remarkably boost the estimation precision, regardless of RWA or non-RWA cases. This is good news for a practical quantum sensing protocol, because the actual noisy environment is complicated and non-Markovian, compared with the oversimplified memoryless approximation used in certain theoretical treatments. We also reveal that the pure dephasing is not the optimal decoherence mechanism to obtain the maximum estimation precision. By introducing a perpendicular qubit-environment interaction, the estimation performance can be improved. Furthermore, by adjusting the value of χ to change the weight of the perpendicular interaction in the $\hat{\mathcal{S}}$ operator, one can attain a larger value of QFI. Due to the fact that both the specific forms of $\alpha(t)$ and $\hat{\mathcal{S}}$ play important roles in determining reduced dynamical behavior of the qubit probe, our result implies the noisy parameter estimation precision can be optimized by controlling the decoherence mechanism.

Though these results are achieved in the Ornstein-Uhlenbeck autocorrelation function case, thanks to the rapid development of the HEOM method, our analysis of noisy parameter estimation can be generalized to other autocorrelation functions. For example, as reported in Refs. [62,63,77,78], the HEOM method has been extended to an arbitrary spectral density function as well as finite temperature environment situation. Moreover, it has been reported that the HEOM method can be extended to simulate the dissipative dynamics of a a few-level system embedded in a fermionic environment [53,65,79] or a spin environment [80,81]. It would be very interesting to extrapolate our paper to these more general situations.

Finally, due to the comprehensive utilizations of the qubit-based quantum sensor, our paper provides a means of designing an optimal estimation scheme to characterize a parameter of interest in a noisy environment. The strategy explored in this paper might have certain potential applications in the researches of quantum metrology and quantum sensing.

ACKNOWLEDGMENTS

W.W. wishes to thank Dr. S.-Y. Bai, Prof. H.-G. Luo, and Prof. J.-H. An for many useful discussions. This work is supported by the National Natural Science Foundation of China (Grant No. 11704025).

APPENDIX

In this Appendix, we show how to derive Eq. (6) from the common Schrödinger equation $\partial_t|\Psi_{\rm sb}(t)\rangle = -i\hat{H}|\Psi_{\rm sb}(t)\rangle$. The whole probe-environment Hamiltonian in the interaction picture with respect to the environment reads

$$\hat{H}(t) = \hat{H}_{\rm s} + \hat{\mathcal{S}}\sum_k (g_k\hat{b}_k^\dagger e^{i\omega_k t} + g_k\hat{b}_k e^{-i\omega_k t}). \tag{A1}$$

Substituting $\hat{H}(t)$ into the standard Schrödinger equation, we have

$$\partial_t|\Psi_{\rm sb}(t)\rangle = -i\left[\hat{H}_{\rm s} + \hat{\mathcal{S}}\sum_k g_k\hat{b}_k^\dagger e^{i\omega_k t} + g_k\hat{b}_k e^{-i\omega_k t}\right]|\Psi_{\rm sb}(t)\rangle. \tag{A2}$$

Then, we employe the Bargmann coherent state $|\mathbf{z}\rangle = \bigotimes_k |z_k\rangle$ with $|z_k\rangle \equiv e^{z_k\hat{b}_k^\dagger}|0_k\rangle$ to reexpress Eq. (A2). By left-multiplying the Bargmann coherent state $\langle\mathbf{z}|$ on both sides of Eq. (A2), one can find

$$\begin{aligned}\partial_t\langle\mathbf{z}|\Psi_{\rm sb}(t)\rangle = &-i\hat{H}_{\rm s}\langle\mathbf{z}|\Psi_{\rm sb}(t)\rangle \\ &- i\hat{\mathcal{S}}\langle\mathbf{z}|\left[\sum_k g_k\hat{b}_k^\dagger e^{i\omega_k t} + g_k\hat{b}_k e^{-i\omega_k t}\right]|\Psi_{\rm sb}(t)\rangle.\end{aligned} \tag{A3}$$

Next, using the following properties of the Bargmann coherent state,

$$\hat{b}_k|z_k\rangle = z_k|z_k\rangle, \quad \hat{b}_k^\dagger|z_k\rangle = \frac{\partial}{\partial z_k}|z_k\rangle, \tag{A4}$$

Eq. (A3) can be simplified to

$$\partial_t|\psi_t(\mathbf{z}^*)\rangle = \left[-i\hat{H}_{\rm s} + \hat{\mathcal{S}}\mathbf{z}_t^* - i\hat{\mathcal{S}}\sum_k g_k e^{-i\omega_k t}\frac{\partial}{\partial z_k^*}\right]|\psi_t(\mathbf{z}^*)\rangle,$$

where $\mathbf{z}_t \equiv i\sum_k g_k z_k e^{-i\omega_k t}$. The term $\frac{\partial}{\partial z_k^*}|\psi_t(\mathbf{z}^*)\rangle$ can be cast as a functional derivative by making use of the functional chain rule [82,83]:

$$\frac{\partial}{\partial z_k^*}|\psi_t(\mathbf{z}^*)\rangle = \int_0^t d\tau\,\frac{\partial\mathbf{z}_\tau^*}{\partial z_k^*}\frac{\delta}{\delta\mathbf{z}_\tau^*}|\psi_t(\mathbf{z}^*)\rangle. \tag{A5}$$

Finally, we have

$$\frac{\partial}{\partial t}|\psi_t(\mathbf{z}^*)\rangle = -i\hat{H}_s|\psi_t(\mathbf{z}^*)\rangle + \hat{\mathcal{S}}\mathbf{z}_t^*|\psi_t(\mathbf{z}^*)\rangle - \hat{\mathcal{S}}\int_0^t d\tau \sum_k g_k^2 e^{-i\omega_k(t-\tau)}\frac{\delta}{\delta \mathbf{z}_\tau^*}|\psi_t(\mathbf{z}^*)\rangle,$$

which reproduces Eq. (6) in the main text. Therefore, by defining the stochastic process $\mathbf{z}_t$ which originates from environmental degrees of freedom, the standard Schrödinger equation can be converted into the stochastic quantum state diffusion equation.

[1] M. Tse *et al.*, Quantum-Enhanced Advanced LIGO Detectors in the Era of Gravitational-Wave Astronomy, Phys. Rev. Lett. **123**, 231107 (2019).

[2] F. Acernese *et al.*, Increasing the Astrophysical Reach of the Advanced Virgo Detector Via the Application of Squeezed Vacuum States of Light, Phys. Rev. Lett. **123**, 231108 (2019).

[3] M. Xu and M. J. Holland, Conditional Ramsey Spectroscopy with Synchronized Atoms, Phys. Rev. Lett. **114**, 103601 (2015).

[4] M. Xu, D. A. Tieri, E. C. Fine, J. K. Thompson, and M. J. Holland, Synchronization of Two Ensembles of Atoms, Phys. Rev. Lett. **113**, 154101 (2014).

[5] L. A. Correa, M. Mehboudi, G. Adesso, and A. Sanpera, Individual Quantum Probes for Optimal Thermometry, Phys. Rev. Lett. **114**, 220405 (2015).

[6] K. V. Hovhannisyan and L. A. Correa, Measuring the temperature of cold many-body quantum systems, Phys. Rev. B **98**, 045101 (2018).

[7] Q. Bouton, J. Nettersheim, D. Adam, F. Schmidt, D. Mayer, T. Lausch, E. Tiemann, and A. Widera, Single-Atom Quantum Probes for Ultracold Gases Boosted by Nonequilibrium Spin Dynamics, Phys. Rev. X **10**, 011018 (2020).

[8] D. A. Herrera-Martí, T. Gefen, D. Aharonov, N. Katz, and A. Retzker, Quantum Error-Correction-Enhanced Magnetometer Overcoming the Limit Imposed by Relaxation, Phys. Rev. Lett. **115**, 200501 (2015).

[9] I. Baumgart, J.-M. Cai, A. Retzker, M. B. Plenio, and Ch. Wunderlich, Ultrasensitive Magnetometer Using a Single Atom, Phys. Rev. Lett. **116**, 240801 (2016).

[10] S. Bhattacharjee, U. Bhattacharya, W. Niedenzu, V. Mukherjee, and A. Dutta, Quantum magnetometry using two-stroke thermal machines, New J. Phys. **22**, 013024 (2020).

[11] T. Nagata, R. Okamoto, J. L. O'Brien, K. Sasaki, and S. Takeuchi, Beating the standard quantum limit with four-entangled photons, Science **316**, 726 (2007).

[12] Y.-Q. Zou, L.-N. Wu, Q. Liu, X.-Yu. Luo, S.-F. Guo, J.-H. Cao, M. K. Tey, and L. You, Beating the classical precision limit with spin-1 Dicke states of more than 10,000 atoms, Proc. Natl. Acad. Sci. USA **115**, 6381 (2018).

[13] J. Zhang, M. Um, D. Lv, J.-N. Zhang, L.-M. Duan, and K. Kim, Noon States of Nine Quantized Vibrations in Two Radial Modes of a Trapped Ion, Phys. Rev. Lett. **121**, 160502 (2018).

[14] S. A. Haine and S. S. Szigeti, Quantum metrology with mixed states: When recovering lost information is better than never losing it, Phys. Rev. A **92**, 032317 (2015).

[15] C. M. Caves, Quantum-mechanical noise in an interferometer, Phys. Rev. D **23**, 1693 (1981).

[16] S. P. Nolan, S. S. Szigeti, and S. A. Haine, Optimal and Robust Quantum Metrology Using Interaction-Based Readouts, Phys. Rev. Lett. **119**, 193601 (2017).

[17] C. L. Degen, F. Reinhard, and P. Cappellaro, Quantum sensing, Rev. Mod. Phys. **89**, 035002 (2017).

[18] L. Pezzè, A. Smerzi, M. K. Oberthaler, R. Schmied, and P. Treutlein, Quantum metrology with nonclassical states of atomic ensembles, Rev. Mod. Phys. **90**, 035005 (2018).

[19] C. W. Helstrom, Quantum Detection and Estimation Theory (1976).

[20] A. S. Holevo, *Probabilistic and Statistical Aspects of Quantum Theory* (1982).

[21] J. Liu, H. Yuan, X.-M. Lu, and X. Wang, Quantum Fisher information matrix and multiparameter estimation, J. Phys. A: Math. Theor. **53**, 023001 (2019).

[22] J. Ma and X. Wang, Fisher information and spin squeezing in the Lipkin-Meshkov-Glick model, Phys. Rev. A **80**, 012318 (2009).

[23] Z. Sun, J. Ma, X.-M. Lu, and X. Wang, Fisher information in a quantum-critical environment, Phys. Rev. A **82**, 022306 (2010).

[24] W. Wu and J.-B. Xu, Geometric phase, quantum Fisher information, geometric quantum correlation and quantum phase transition in the cavity-Bose–Einstein-condensate system, Quantum Inf. Proc. **15**, 3695 (2016).

[25] T.-L. Wang, L.-N. Wu, W. Yang, G.-R. Jin, N. Lambert, and F. Nori, Quantum Fisher information as a signature of the superradiant quantum phase transition, New J. Phys. **16**, 063039 (2014).

[26] F. Fröwis, Kind of entanglement that speeds up quantum evolution, Phys. Rev. A **85**, 052127 (2012).

[27] M. M. Taddei, B. M. Escher, L. Davidovich, and R. L. de Matos Filho, Quantum Speed Limit for Physical Processes, Phys. Rev. Lett. **110**, 050402 (2013).

[28] S. Deffner and S. Campbell, Quantum speed limits: from Heisenberg's uncertainty principle to optimal quantum control, J. Phys. A: Math. Theor. **50**, 453001 (2017).

[29] X.-M. Lu, X. Wang, and C. P. Sun, Quantum Fisher information flow and non-Markovian processes of open systems, Phys. Rev. A **82**, 042103 (2010).

[30] H. Song, S. Luo, and Y. Hong, Quantum non-Markovianity based on the Fisher-information matrix, Phys. Rev. A **91**, 042110 (2015).

[31] C.-F. Li, G.-C. Guo, and J. Piilo, Non-Markovian quantum dynamics: What does it mean? Europhys. Lett. **127**, 50001 (2019).

[32] A. J. Leggett, S. Chakravarty, A. T. Dorsey, M. P. A. Fisher, A. Garg, and W. Zwerger, Dynamics of the dissipative two-state system, Rev. Mod. Phys. **59**, 1 (1987).

[33] H.-P. Breuer, E.-M. Laine, J. Piilo, and B. Vacchini, Colloquium: Non-Markovian dynamics in open quantum systems, Rev. Mod. Phys. **88**, 021002 (2016).

[34] I. de Vega and D. Alonso, Dynamics of non-Markovian open quantum systems, Rev. Mod. Phys. **89**, 015001 (2017).

[35] R. Demkowicz-Dobrzanski, J. Kolodynski, and M. Guta, The elusive Heisenberg limit in quantum-enhanced metrology, Nat. Commun. **3**, 1063 (2012).

[36] R. Demkowicz-Dobrzański and L. Maccone, Using Entanglement Against Noise in Quantum Metrology, Phys. Rev. Lett. **113**, 250801 (2014).

[37] S. Alipour, M. Mehboudi, and A. T. Rezakhani, Quantum Metrology in Open Systems: Dissipative Cramér-Rao Bound, Phys. Rev. Lett. **112**, 120405 (2014).

[38] N. Mirkin, M. Larocca, and D. Wisniacki, Quantum metrology in a non-Markovian quantum evolution, arXiv:1912.04675.

[39] A. W. Chin, S. F. Huelga, and M. B. Plenio, Quantum Metrology in Non-Markovian Environments, Phys. Rev. Lett. **109**, 233601 (2012).

[40] S. Razavian, C. Benedetti, M. Bina, Y. Akbari-Kourbolagh, and M. G. A. Paris, Quantum thermometry by single-qubit dephasing, European Phys. J. Plus **134**, 284 (2019).

[41] K. Berrada, Non-Markovian effect on the precision of parameter estimation, Phys. Rev. A **88**, 035806 (2013).

[42] Q.-S. Tan, Y. Huang, X. Yin, L.-M. Kuang, and X. Wang, Enhancement of parameter-estimation precision in noisy systems by dynamical decoupling pulses, Phys. Rev. A **87**, 032102 (2013).

[43] Y.-S. Wang, C. Chen, and J.-H. An, Quantum metrology in local dissipative environments, New J. Phys. **19**, 113019 (2017).

[44] C. Benedetti, F. S. Sehdaran, M. H. Zandi, and M. G. A. Paris, Quantum probes for the cutoff frequency of ohmic environments, Phys. Rev. A **97**, 012126 (2018).

[45] F. S. Sehdaran, M. H. Zandi, and A. Bahrampour, The effect of probe-Ohmic environment coupling type and probe information flow on quantum probing of the cutoff frequency, Phys. Lett. A **383**, 126006 (2019).

[46] Y. Tanimura and R. Kubo, Time evolution of a quantum system in contact with a nearly Gaussian-Markovian noise bath, J. Phys. Soc. Jpn. **58**, 101 (1989).

[47] Y. an Yan, F. Yang, Y. Liu, and J. Shao, Hierarchical approach based on stochastic decoupling to dissipative systems, Chem. Phys. Lett. **395**, 216 (2004).

[48] R.-X. Xu and YiJing Yan, Dynamics of quantum dissipation systems interacting with bosonic canonical bath: Hierarchical equations of motion approach, Phys. Rev. E **75**, 031107 (2007).

[49] J. Jin, X. Zheng, and Y. J. Yan, Exact dynamics of dissipative electronic systems and quantum transport: Hierarchical equations of motion approach, J. Chem. Phys. **128**, 234703 (2008).

[50] J. Ma, Z. Sun, X. Wang, and F. Nori, Entanglement dynamics of two qubits in a common bath, Phys. Rev. A **85**, 062323 (2012).

[51] W. Wu and H.-Q. Lin, Effect of bath temperature on the decoherence of quantum dissipative systems, Phys. Rev. A **94**, 062116 (2016).

[52] W. Wu and H.-Q. Lin, Quantum Zeno and anti-Zeno effects in quantum dissipative systems, Phys. Rev. A **95**, 042132 (2017).

[53] W. Wu and M. Liu, Effects of counter-rotating-wave terms on the non-Markovianity in quantum open systems, Phys. Rev. A **96**, 032125 (2017).

[54] D. P. DiVincenzo and D. Loss, Rigorous born approximation and beyond for the spin-boson model, Phys. Rev. B **71**, 035318 (2005).

[55] G. Burkard, Non-Markovian qubit dynamics in the presence of $1/f$ noise, Phys. Rev. B **79**, 125317 (2009).

[56] S. F. Huelga, C. Macchiavello, T. Pellizzari, A. K. Ekert, M. B. Plenio, and J. I. Cirac, Improvement of Frequency Standards with Quantum Entanglement, Phys. Rev. Lett. **79**, 3865 (1997).

[57] P. Hauke, M. Heyl, L. Tagliacozzo, and P. Zoller, Measuring multipartite entanglement through dynamic susceptibilities, Nat. Phys. **12**, 778 (2016).

[58] K. C. McCormick, J. Keller, S. C. Burd, D. J. Wineland, A. C. Wilson, and D. Leibfried, Quantum-enhanced sensing of a single-ion mechanical oscillator, Nature (London) **572**, 86 (2019).

[59] J. F. Haase, A. Smirne, J. Kołodyński, R. Demkowicz-Dobrzański, and S. F. Huelga, Fundamental limits to frequency estimation: A comprehensive microscopic perspective, New J. Phys. **20**, 053009 (2018).

[60] K. Bai, Z. Peng, H.-G. Luo, and J.-H. An, Retrieving Ideal Precision in Noisy Quantum Optical Metrology, Phys. Rev. Lett. **123**, 040402 (2019).

[61] D. Tamascelli, C. Benedetti, H.-P. Breuer, and M. G. A. Paris, Quantum probing beyond pure dephasing, New J. Phys. **22**, 083027 (2020).

[62] W. Wu, Realization of hierarchical equations of motion from stochastic perspectives, Phys. Rev. A **98**, 012110 (2018).

[63] W. Wu, Stochastic decoupling approach to the spin-boson dynamics: Perturbative and nonperturbative treatments, Phys. Rev. A **98**, 032116 (2018).

[64] D. Suess, A. Eisfeld, and W. T. Strunz, Hierarchy of Stochastic Pure States for Open Quantum System Dynamics, Phys. Rev. Lett. **113**, 150403 (2014).

[65] D. Suess, W. T. Strunz, and A. Eisfeld, Hierarchical equations for open system dynamics in fermionic and bosonic environments, J. Stat. Phys. **159**, 1408 (2015).

[66] S. Nakajima, On Quantum Theory of Transport Phenomena: Steady Diffusion, Prog. Theor. Phys. **20**, 948 (1958).

[67] R. Zwanzig, Ensemble method in the theory of irreversibility, J. Chem. Phys. **33**, 1338 (1960).

[68] W. Wu and W.-L. Zhu, Heat transfer in a nonequilibrium spin-boson model: A perturbative approach, Ann. Phys. (NY) **418**, 168203 (2020).

[69] H. Z. Shen, M. Qin, X.-M. Xiu, and X. X. Yi, Exact non-Markovian master equation for a driven damped two-level system, Phys. Rev. A **89**, 062113 (2014).

[70] B. Bellomo, R. Lo Franco, and G. Compagno, Non-Markovian Effects on the Dynamics of Entanglement, Phys. Rev. Lett. **99**, 160502 (2007).

[71] J.-G. Li, J. Zou, and B. Shao, Non-Markovianity of the damped Jaynes-Cummings model with detuning, Phys. Rev. A **81**, 062124 (2010).

[72] W. Wu and J.-Q. Cheng, Coherent dynamics of a qubit–oscillator system in a noisy environment, Quantum Inf. Proc. **17**, 300 (2018).

[73] S. C. Hou, X. X. Yi, S. X. Yu, and C. H. Oh, Alternative non-markovianity measure by divisibility of dynamical maps, Phys. Rev. A **83**, 062115 (2011).

[74] K.-W. Sun, Y. Fujihashi, A. Ishizaki, and Y. Zhao, A variational master equation approach to quantum dynamics with off-diagonal coupling in a sub-ohmic environment, J. Chem. Phys. **144**, 204106 (2016).

[75] Y. M. Galperin, B. L. Altshuler, J. Bergli, and D. V. Shantsev, Non-Gaussian Low-Frequency Noise as a Source of Qubit Decoherence, Phys. Rev. Lett. **96**, 097009 (2006).

[76] X. Cai and Y. Zheng, Non-Markovian decoherence dynamics in nonequilibrium environments, J. Chem. Phys. **149**, 094107 (2018).

[77] Z. Tang, X. Ouyang, Z. Gong, H. Wang, and J. Wu, Extended hierarchy equation of motion for the spin-boson model, J. Chem. Phys. **143**, 224112 (2015).

[78] C. Duan, Z. Tang, J. Cao, and J. Wu, Zero-temperature localization in a sub-ohmic spin-boson model investigated by an extended hierarchy equation of motion, Phys. Rev. B **95**, 214308 (2017).

[79] H.-D. Zhang, L. Cui, H. Gong, R.-X. Xu, X. Zheng, and Y. J. Yan, Hierarchical equations of motion method based on fano spectrum decomposition for low temperature environments, J. Chem. Phys. **152**, 064107 (2020).

[80] C.-Yu. Hsieh and J. Cao, A unified stochastic formulation of dissipative quantum dynamics. I. Generalized hierarchical equations, J. Chem. Phys. **148**, 014103 (2018).

[81] C.-Yu. Hsieh and J. Cao, A unified stochastic formulation of dissipative quantum dynamics. II. Beyond linear response of spin baths, J. Chem. Phys. **148**, 014104 (2018).

[82] L. Diósi and W. T. Strunz, The non-Markovian stochastic Schrödinger equation for open systems, Phys. Lett. A **235**, 569 (1997).

[83] W. T. Strunz, The Brownian motion stochastic Schrödinger equation, Chem. Phys. **268**, 237 (2001).